

Flaw tolerance in ceramics with rising crack resistance characteristics

STEPHEN J. BENNISON*, BRIAN R. LAWN

Ceramics Division, National Institute of Standards and Technology, Gaithersburg, Maryland 20899, USA

The stabilizing influence of increasing toughness with crack size associated with a cumulative closure-stress process (*R*-curve, or *T*-curve) on the strength properties of brittle ceramic materials is analysed. Three strength-controlling flaw types are examined in quantitative detail: microcracks with closure-stress history through both the initial formation and the extension in subsequent strength testing; microcracks with closure stresses active only during the subsequent extension; spherical pores. Using a polycrystalline alumina with pronounced *T*-curve behaviour as a case study, it is demonstrated that the strength is insensitive to a greater or lesser extent on the initial size of the flaw, i.e. the material exhibits the quality of "flaw tolerance". This insensitivity is particularly striking for the flaws with full closure-stress history, with virtually total independence on initial size up to some 100 μm ; for the flaws with only post-evolutionary exposure to the closure elements the effect is less dramatic, but the strength characteristics are nevertheless significantly more insensitive to initial flaw size than their counterparts for materials with single-value toughnesses. The implications of these results to engineering design methodologies, as expressed in conventional *R*-curve constructions, and to processing strategies for tailoring materials with optimal crack resistance properties, are discussed.

1. Introduction

The mechanical characterization of ceramics continues to be based in large part on the traditional notion of a single-valued crack resistance *R*, (or toughness, *T*)[†]. An explicit prediction of any theory of strength based on invariant *R* is that failure should occur spontaneously from some pre-existent ("Griffith") flaw when a critical applied stress is reached, such that the strength varies inversely with the flaw size. This prediction is the cornerstone of nearly all non-destructive evaluation of structural ceramics. It has resulted in a strong movement toward a processing philosophy of flaw elimination [1–5], in which systematic efforts are made to remove all potentially severe flaws. It is, therefore, not difficult to understand why "flaw sensitivity" has remained the most pervasive concept in the entire theory of the strength of ceramics.

The recent realization that many ceramics display an increasing resistance with continued crack extension [6], so-called *R*-curve (or *T*-curve) behaviour, requires that this philosophy be re-examined. Materials with significant *R*-curves do not fail spontaneously; rather, the critical flaw first grows stably, often over a considerable distance, before failure ensues [6–12]. This enhanced stability imparts a certain "flaw

tolerance" to the material, because it is the final, not the initial, size that determines the instability. Such tolerance is of great benefit to the structural designer, because of a tendency to increased reliability (increased Weibull modulus [13, 14]) coupled with a reduced sensitivity to subsequent damage in service [7]. It also offers the attractive prospect of early detection by non-destructive evaluation [11]. Most importantly, perhaps, it reduces the onus on the ceramics processor to fabricate full-density and defect-free materials.

One of the most useful methodologies for examining the influence of *R*-curve behaviour in the context of flaw instability is that of indentation-strength testing, where the strength, σ_m , is determined as a function of indentation load, *P* [7, 11, 12]. The *R*-curve is manifest as a deviation of σ_m from the classical $P^{-1/3}$ dependency for materials with fixed toughness to a distinctive plateau at low indentation loads. By deconvoluting the $\sigma_m(P)$ data set, the *R*-curve can be extracted [12]. For materials with strong *R*-curve characteristics the low-load plateau often appears to correspond to the strength for failure from processing defects [7]. Despite this demonstrated correspondence there is a widespread perception in the ceramics fracture mechanics community that indentation flaws, by virtue of their

*Guest Scientist, on leave from the Department of Materials Science and Engineering, Lehigh University, Bethlehem, Pennsylvania 18015, USA.

[†]The quantities *R* and *T* are interchangeable measures of toughness for ceramics, related in the Griffith–Irwin fracture mechanics by $T = [RE/(1 - \nu^2)]^{1/2}$ for cracks in plane strain, with *E* Young's modulus and ν Poisson's ratio; *R* is the crack resistance in the equilibrium relation $G_c = R$, where *G* is the mechanical-energy-release rate; *T* is the cohesion-intensity factor in the equivalent relation $K_{Ic} = T$, where *K* is the stress-intensity factor. Accordingly, we shall use the terms "*R*-curve" and "*T*-curve" interchangeably throughout this paper.

“artificial” origin, cannot be representative of the natural flaw population; and, therefore, that the latter are not subject to the stabilizing influence of the R -curve.

In this paper we examine the effect of R -curve characteristics on the strength response for some well-defined natural flaw types: sharp microcracks of some grain-facet dimensions with a full R -curve history; the same but without any R -curve history prior to extension; relatively large-scale processing pores. We use indentation-strength data on a specific coarse-grained alumina to establish the toughness characteristics, and invoke a basic R -curve instability condition to determine the variation of strength with initial flaw size for the various flaw types in this same material. The R -curve mechanism in our selected material is identifiable as grain-localized bridging behind the crack tip [9–12, 15]; however, our statements concerning the mechanics of flaw response will be of a general nature. It will be shown that the natural flaw types do indeed exhibit the same kind of tolerance as their artificial indentation counterparts. In arriving at this conclusion we shall dwell on some of the pitfalls that can arise from widely used R -curve constructions that represent the flaw size as a negative intercept of the applied loading function on the crack-size coordinate.

2. Fracture mechanics for flaws in materials with T -curve characteristics

2.1. General conditions for crack equilibrium and stability

We begin by defining a general net stress intensity factor, K , for a uniformly stressed equilibrium crack in a material with R -curve characteristics [6]. We write it as the sum of two terms, an external uniform applied stress term, K_a , and an internal microstructure-associated closure stress term, K_μ

$$K(c) = K_a(c) + K_\mu(c) = T_0 \quad (1a)$$

where T_0 is an intrinsic toughness, and c is the crack length. Or, alternatively,

$$K_a(c) = T_0 + T_\mu(c) = T(c) \quad (1b)$$

where $T_\mu = -K_\mu$ may be regarded as a positive contribution to the toughness. With this definition of a net toughness, T (the stress intensity equivalent, $K_c = T$, of the resistance term associated with the mechanical energy release rate, $G_c = R$), we adopt the term “ T -curve” to describe the size-dependent resistance characteristic.

Consider now the condition for instability [6]. For $T_0 = \text{constant}$ we require the condition

$$dK/dc \geq 0 \quad (2a)$$

to be satisfied in Equation 1a, or, equivalently,

$$dK_a/dc \geq dT/dc \quad (2b)$$

in Equation 1b. This latter is the tangency condition in the familiar R -curve construction.

We now consider the micromechanics of failure for three different flaw types in a material with T -curve due to grain-localized bridging at the crack interface,

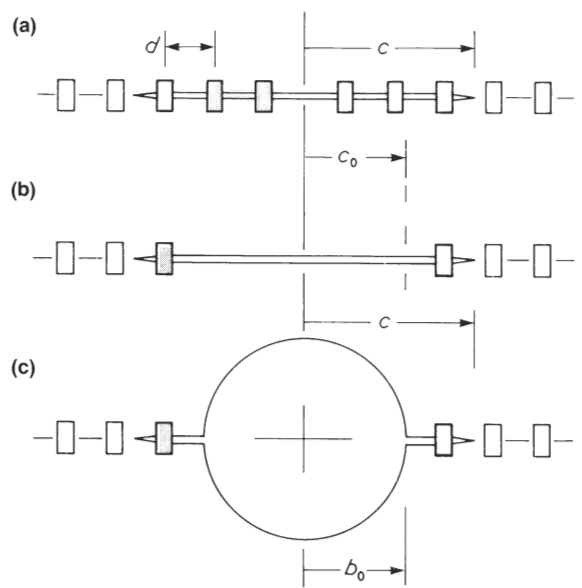


Figure 1 Schematic drawing of flaw types considered in this study: (a) microcracks with full T -curve history, i.e. subject to bridging in initial evolution to $c = c_0$ as well as in subsequent extension at $c > c_0$; (b) microcracks without any T -curve history in evolution to $c = c_0$ prior to extension, but subject to T -curve in subsequent extension $c > c_0$; (c) pores subject to T -curve in extension $c > b_0$. Squares represent bridging grains, mean separation d ; shaded squares are activated bridges; open squares are potential bridges.

a mechanism identified as pertinent to a wide range of non-transforming ceramics [9, 15].

2.2. Microcracks with full T -curve history

Consider first a sharp-crack flaw whose inception and subsequent evolution takes place entirely in the interfacial closure-stress field responsible for the T -curve, Fig. 1a. This might be expected to be a most common state for microcracks with histories unfavourable to the relaxation or destruction of the attendant bridging elements; e.g. flaws developed during the final stages of, or even after, processing. We seek to characterize the response of this flaw type in a subsequent strength test, and thence to determine the dependence of the strength on the “initial” (pre-test) microcrack size, c_0 .

Start with the applied stress term, K_a . For a flaw normal to the applied tensile stress this term has the familiar dependence on the crack size, c [6]

$$K_a(c) = \psi \sigma_a c^{1/2} \quad (c \geq c_0) \quad (3)$$

where ψ is a geometrical constant ($= 2/\pi^{1/2}$ for penny cracks).

The K_μ term is derived from the mechanics of crack-interface bridging for penny-shaped cracks [12]. As the crack begins to extend from the initial flaw, bridging elements are activated over the entire area of the crack beyond intersection with the first bridge at $c = d$, i.e. over most of the initial, as well as all of the subsequent area regardless of the value of c_0 . The attendant restraint stabilizes the crack growth. The build-up of interfacial surface traction prevails until, at a crack size $c = c_*$, the bridges furthestmost behind the advancing tip begin to rupture, at which point the bridge configuration translates with the tip in steady state. Derivation of the K_μ term thereby involves integration of the underlying (continuum approximation)

stress-separation function for the bridging elements within $d \leq c \leq c_*$ [10]. Because this bridging term is negative, we adopt the T_μ notation of Equation 1b, thus [12]

$$T_\mu(c) = 0, \quad (c < d) \quad (4a)$$

$$T_\mu(c) = (T_\infty - T_0) \times \{1 - \{1 - [c_*(c^2 - d^2)/c(c_*^2 - d^2)]^{1/2}\}^3\}, \quad (d < c < c_*) \quad (4b)$$

$$T_\mu(c) = T_\infty - T_0, \quad (c > c_*) \quad (4c)$$

with T_∞ the steady-state value of T .

Let us emphasize that the derivation of this particular relation, or even the identification of bridging as the particular T -curve mechanism, are not issues here; we use Equation 4 only as a formula for representing the experimentally determined results for our chosen alumina test material. Any other analytical expression that fits the T -curve data would serve equally well to demonstrate the tolerance factor in the strength characteristics.

2.3. Microcracks without full T -curve history

Now consider our second microcrack-type flaw, of the same initial size, c_0 , but without any (pre-test) history of interfacial bridging, Fig. 1b. Such could be the case if bridges were never to be given the chance to form in the first place (e.g. flaws associated with incomplete densification at an early stage of sintering, grain-boundary triple points), or if any post-fabrication mechanical, thermal or chemical interaction were to destroy existing (i.e. post-evolutionary) bridges.

The applied stress term, $K_a(c)$, is identical to that of Equation 3. However, the microstructure-associated $T_\mu(c)$ term differs slightly from Equation 4, by virtue of the fact that the bridging stresses are operative only over the area of the extended (not the initial) crack. In this case the T -curve is displaced along the c -axis, corresponding to integration of the stress-separation function for the bridging elements between $c_0 + d \leq c \leq c_0 + c_*$ [10]. The expressions for T_μ may thus be obtained by replacing d in Equation 4 with $c_0 + d$ and c_* by $c_0 + c_*$

$$T_\mu(c) = 0, \quad (c < c_0 + d) \quad (5a)$$

$$T_\mu(c) = (T_\infty - T_0)[1 - \{1 - \{[c_0 + c_*(c^2 - (c_0 + d)^2)]/c[(c_0 + c_*)^2 - (c_0 + d)^2]^{1/2}\}^3\}], \quad (c_0 + d < c < c_0 + c_*) \quad (5b)$$

$$T_\mu(c) = T_\infty - T_0, \quad (c > c_0 + c_*) \quad (5c)$$

which now explicitly involves flaw size, c_0 . We emphasize here that this T -curve displacement is not equivalent to a simple shift in origin along the c -axis; i.e. the function $T_\mu(\Delta c)$, where $\Delta c = c - c_0$, is not invariant.

2.4. Crack extension from pores

For our third flaw type, consider a spherical pore of radius b_0 , from which annular microcracks extend on a diametral plane normal to the subsequently applied tensile field, Fig. 1c. The terminology b_0 is adopted here to distinguish this kind of defect from a sharp

crack (a distinction overlooked by some). Pores are the most common manifestation of processing in which full density is not realised.

The applied stress term for the pore is no longer of the simple form given in Equation 3. Note that the true crack size in this case is not c but $c - b_0$. The consequent reduction in effectiveness of the pore as a strength-degrading flaw is negated somewhat by a stress-concentrating capacity. Accordingly, $K_a(c)$ is modified as follows

$$K_a(c) = \psi \sigma_a (c - b_0)^{1/2} f(b_0/c) \quad (c \geq b_0) \quad (6)$$

where the modifying function $f(b_0/c)$ is [16] (neglecting free surface effects at $c = b_0$)

$$f(b_0/c) = (1 + b_0/c)^{1/2} \{1 + (1/2)(b_0/c)^2 + [3/(7 - 5\nu)](b_0/c)^4\}, \quad (c \geq b_0) \quad (7)$$

with ν Poisson's ratio. Note that at $c \geq b_0$, $f \rightarrow 1$, as required for Equation 7 to restore to Equation 3. As c decreases toward b_0 , on the other hand, f becomes increasingly greater than unity, indicative of the stress-concentration effect. Again, there are more sophisticated expressions for $f(c/b_0)$, but the numerical accuracy of Equation 7 is not central to our argument.

For the microstructure-associated $K_\mu(c)$ term we may retain Equation 5 above as for microcracks without T -curve history, but with b_0 replacing c_0 (again in the approximation of negligible free surface effects at $c = b_0$)

$$T_\mu(c) = 0, \quad (c < b_0 + d) \quad (8a)$$

$$T_\mu(c) = (T_\infty - T_0)[1 - \{1 - \{(b_0 + c_*(c^2 - (b_0 + d)^2)]/c[b_0 + c_*)^2 - (b_0 + d)^2]^{1/2}\}^3\}], \quad (b_0 + d < c < b_0 + c_*) \quad (8b)$$

$$T_\mu(c) = T_\infty - T_0, \quad (c > b_0 + c_*) \quad (8c)$$

so that initial flaw size is again a factor. Again, we note that the function $T_\mu(\Delta c)$, where $\Delta c = c - b_0$, is not invariant.

3. Calculation of strength – flaw-size relations: case study on a polycrystalline alumina

3.1. A model alumina material

Let us now investigate the above formulations for an alumina with relatively pronounced T -curve (R -curve) characteristics associated with the bridging mechanism. The appropriate parameters needed in order to specify T_μ in Equation 3 for this material have been evaluated from the indentation-strength, $\sigma_m(P)$, data shown in Fig. 2 [12]. We note the distinct plateau in these data, indicative of the strong T -curve influence referred to earlier. This plateau corresponds closely to the strength level for breaks from natural flaws (including unindented specimens, and indented specimens whose failures did not originate at the contact site). The material is polycrystalline with an average grain size $20 \mu\text{m}$ (Vistal grade, grain size $20 \mu\text{m}$, $< 0.1\%$ impurity, Coors Ceramics Co., Colorado). It has a strong tendency to intergranular

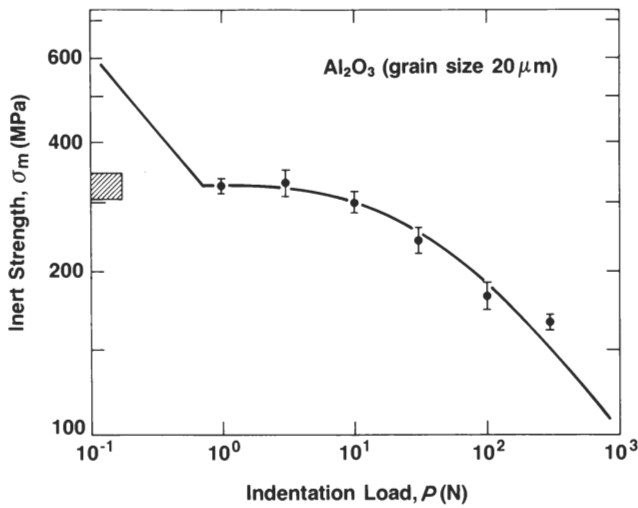


Figure 2 Indentation-strength data for polycrystalline alumina (from [7]). Data points are means and standard deviations for breaks at indentation flaws formed at different loads. Hatched area at left is strength for breaks from natural flaws. Curve through data is fit used to deconvolute T -curve.

fracture [7], so that the intrinsic toughness, T_0 , identifies with the grain-boundary fracture resistance. The specimens were broken in their as-fired state, so that extrinsic machining or polishing flaws might be avoided. However, they contain some readily observable processing defects: microcracks up to $50 \mu\text{m}$ long (≈ 2 to 3 grain facet lengths) and occasional large pores up to $100 \mu\text{m}$ radius, examples of which are shown in Fig. 3. These defects have been identified as the failure sites for breaks of unindented specimens (or, at low contact loads, of some indented specimens).

Accordingly, we plot the applied stress $K_a(c)$ function and equilibrium $T(c)$ function of Equation 1b for the three flaw types, in Figs 4 to 6. The crack coordinate is plotted as $c^{1/2}$ in these figures so that $K_a(c)$ for the microcrack-type flaws might be represented in the usual way as straight lines with slope proportional to applied stress. The T -curves have the same form for each of the different flaw types, with lateral displacements along the abscissa depending on the effective initial flaw size. The range in c over which the T -curve rises for this alumina may be taken as a measure of the

large zone lengths ($c - d$) over which the stabilizing effect of the restraining forces can be realized in non-transforming ceramics.

3.2. Microcracks: full T -curve history

Consider first the T curve construction for microcrack-like flaws with full T -curve history, Fig. 4. In this case the $T(c)$ function, Equation 4, is independent of initial flaw size, c_0 . The actual critical condition for failure, Equation 2b, corresponding to the tangency condition $\sigma_a = \sigma_m = \sigma_3$ in the diagram, also shows an independence on c_0 , but only within the size range $c'_0 \leq c_0 \leq c''_0$. For the particular value of c_0 illustrated the flaw first "pops in" unstably to the intersection point along the "loading line" at $\sigma_a = \sigma_2$ on the rising branch of the T -curve, and thereafter grows stably up the curve until the critical unstable configuration $c = c_m = c''_0$ is reached at $\sigma_a = \sigma_m^p = \sigma_3$ (superscript P denoting plateau value). This may be regarded as an "activated" instability. For $c_0 < c'_0$ the instability condition $\sigma_a = \sigma_m$ occurs at a higher applied stress level, e.g. σ_4 ; conversely, for $c_0 > c''_0$ at lower σ_a , e.g. σ_2 or (for very large c_0) σ_1 . In these latter cases the instability is "spontaneous". With such a construction we can determine (at least numerically) the functional dependence of σ_m on c_0 over as wide a range of flaw size as we please.

3.3. Microcracks: no previous T -curve history

Consider next the construction for the same microcrack-like flaws, but without T -curve history. As indicated above, the influence of initial flaw size c_0 is now manifest as a shift in the $T(c)$ function, Equation 5, along the c -axis, without any effect on the $K_a(c)$ function. We plot $T(c)$ for $c_0 = 0$ (i.e. equivalent to flaw with full T -curve history, Equation 4), $50 \mu\text{m}$ (corresponding to the approximate microcrack size actually observed, Section 3.1) and $500 \mu\text{m}$ (an extreme value approaching "macroscopic" crack dimensions) in Fig. 5. We include $K_a(c)$ loading lines only at the tangency configurations. Note now that even within the flaw size range $c'_0 \leq c_0 \leq c''_0$ (a condition always well satisfied for the 50 and $500 \mu\text{m}$ flaws represented in Fig. 5) this tangency configuration is not independent

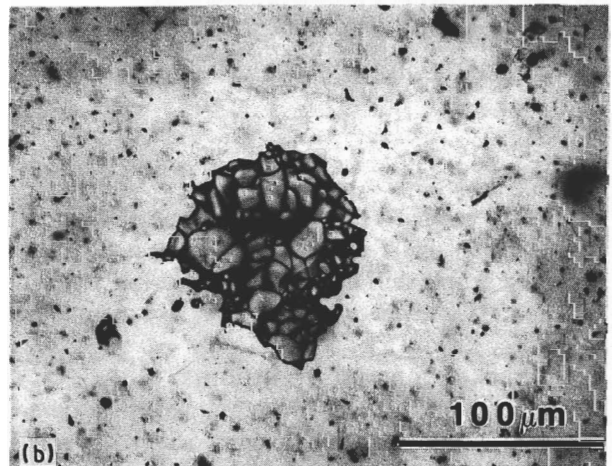
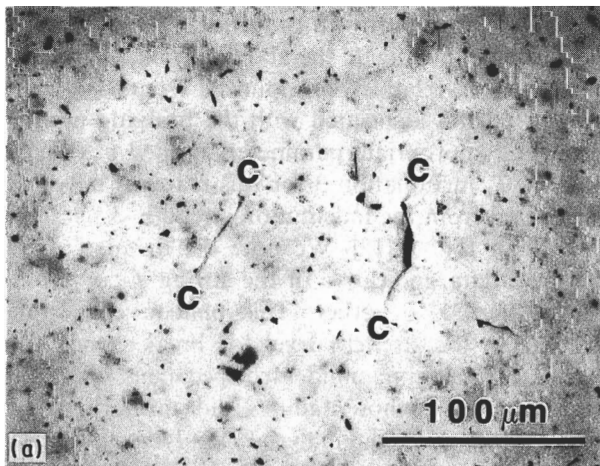


Figure 3 Micrographs of processing flaws in the same alumina as represented in Fig. 2: (a) microcracks (C), (b) large pore. Optical, transmitted light.

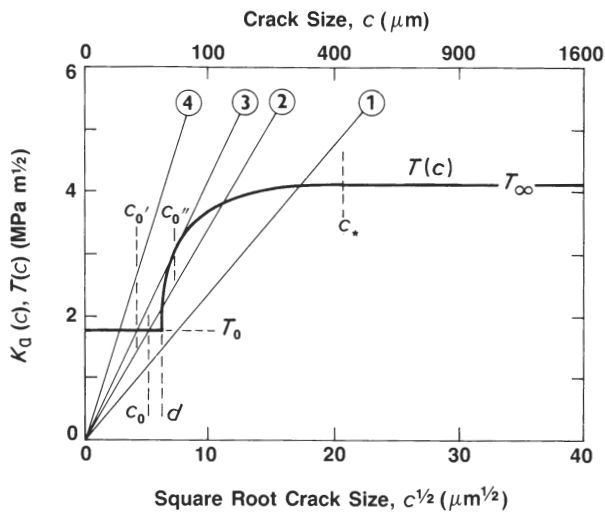


Figure 4 T -curve construction for alumina material in Fig. 2: microcrack flaws with full T -curve history. Lines 1, 2, 3, 4 correspond to increasing σ_a in $K_a(c)$ function, Equation 3. $T(c)$ function from Equation 4 using parameters evaluated from Fig. 2 ($T_0 = 1.73 \text{ MPa m}^{1/2}$, $T_\infty = 4.08 \text{ MPa m}^{1/2}$, $d = 40 \mu\text{m}$, $c_* = 420 \mu\text{m}$ [12]). Tangency condition at curve 3 defines strength $\sigma_a = \sigma_m = 305 \text{ MPa}$ for flaws with initial size in range $c_0' \leq c_0 \leq c_0''$

of c_0 ; i.e. the slope of the $K_a(c)$ line, which determines $\sigma_a = \sigma_m$, differs from curve to curve. Nevertheless, not only is the failure still activated, but the stable growth stage prior to final instability is actually enhanced (the tangency point lies further up the T -curve at the two larger values of c_0). Accordingly, the tolerance characteristic imparted by the T -curve will be far from lost, especially where the range of the T -curve greatly exceeds the range of flaw sizes, as is the case for our material in Fig. 5. Again, it is a straightforward matter to determine the functional dependence of σ_m on c_0 from this construction.

3.4. Pores

Finally, consider the construction for the pore-like flaws. Now both the $T(c)$ function, Equation 8, and the $K_a(c)$ function, Equations 6 and 7, are dependent on the initial flaw size, b_0 . We plot these two functions

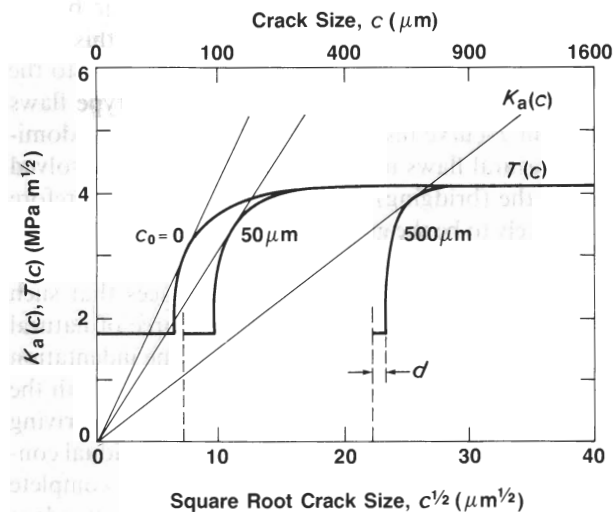


Figure 5 As for Fig. 4, but for microcrack flaws without T -curve history over initial evolution length, c_0 . $T(c)$ curves correspond to $c_0 = 0$ (reference curve from Fig. 4), 50 and 500 μm in Equation 5. $K_a(c)$ lines are for tangency condition at each T -curve.

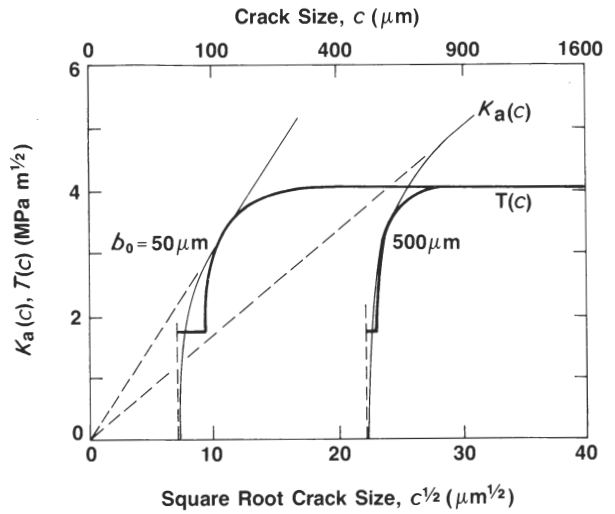


Figure 6 As for Fig. 5, but for pores of sizes $b_0 = 50$ and $500 \mu\text{m}$. $T(c)$ curves from Equation 8, $K_a(c)$ curves from Equations 6 and 7. Note deviation of $K_a(c)$ below $c^{1/2}$ dependence (dashed lines) at small c , with zero cut-off at $c = b_0$. (Note also that T and K_a crack functions are definable only at $c \geq b_0$ for this defect.)

for $b_0 = 50$ and $500 \mu\text{m}$ in Fig. 6 (cf. flaw sizes in Section 3.3); for $K_a(c)$ we include plots for equivalent cracks, $b_0 = c_0$ in Equation 3, as the dashed lines. The modifying effect of the effective reduction in crack length (from c to $c - b_0$) associated with the pore is apparent as a pronounced deviation below a linear $K_a(c)$ plot, with cut-off at small crack extensions. However, the stabilizing effect of the T -curve is sufficiently strong that this modification has little noticeable influence on the tangency condition, except at unusually large pore sizes (such as the $500 \mu\text{m}$ pore in Fig. 6). Again, the tangency configuration depends on the size of the history-dependent flaw. Note that for this tangency condition to represent the strength configuration it is necessary only that the pore should be circumscribed by a pre-existent annular starter crack, Δc , a few micrometres in dimension (i.e. considerably less than a grain facet length in our material), such that the requirement $c_0' \leq b_0 + \Delta c \leq c_0''$ (cf. Fig. 4) is

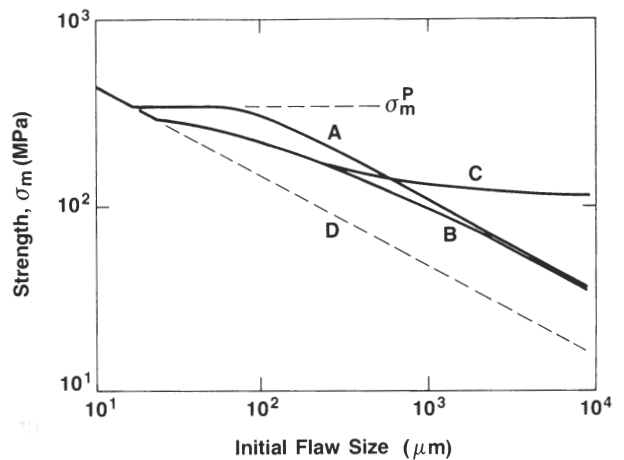


Figure 7 Predicted strength plotted against initial flaw size (c_0 for microcracks, b_0 for pores) for alumina material in Fig. 2: A, microcracks with full T -curve history; B, microcracks with T -curve influence only after extension from c_0 ; C, pores with T -curve influence after extension from b_0 ; D, microcracks with no influence of T -curve at any stage of growth. Note well-defined plateau level at σ_m^p is fully achieved only by flaw A.

satisfied. In the interest of conservative design we deal with this “worst case” in Section 3.5 below.

3.5. Strength data

Fig. 7 is the resultant plot of the strength against initial flaw size (c_0 or b_0 , whichever is appropriate) for the three flaw types discussed above, indicated as curves A, B and C, respectively. It is evident that the stabilizing influence of the T -curve has produced significant flaw tolerance over the size range 10 to 100 μm (encompassing the range observed in our alumina material, Section 3.1), even if somewhat less pronounced in B and C where bridging is not operative over the initial length. To put these results in perspective, we may compare with the strength characteristics for a hypothetical ceramic with the same material constants as our alumina but without T -curve influence over any of the crack area, extended as well as initial; these characteristics are obtained here by repeating the calculations for sharp microcracks at $T_\mu = 0$ (i.e. with a toughness $T = T_0$) and are plotted as curve D in Fig. 7.

4. Discussion

It has been shown that different flaw types in materials with pronounced T -curve (R -curve) characteristics exhibit the quality of “tolerance” in their associated strength behaviour, to a greater or lesser extent depending on history and geometry. The greatest effect is predicted for those flaws that experience enhanced resistance over their entire area, initial as well as extended. A smaller, but by no means insignificant, effect is predicted for those flaws that experience resistance over only their extended area. This latter point runs counter to traditional thought in the ceramics community where it is presumed that certain flaws, particularly processing defects, are inevitably susceptible to spontaneous failure from their initial configuration. Our results would suggest that in such T -curve materials as the alumina represented in Fig. 7, the improvements in strength gained by eliminating processing flaws much smaller than 100 μm (corresponding to a few bridge spacings) are likely to be minimal.

We have considered just one material (polycrystalline alumina), and just one mechanism (bridging), but the conclusions carry over to any material and any mechanism. It is the form, not the origin, of the T -curve that determines the scale of the effect. (We have recently refined the detailed form of the T -curve for bridging materials given in Equation 4, but these refinements in no way change the substance of our conclusions here.) Note that there are two features of the T -curve that need to be maximized for optimum tolerance, the magnitude $T_\infty - T_0$, and the range $c_* - d$. For the alumina considered here the magnitude is modest, $T_\infty/T_0 \approx 2$ to 3, but the range is relatively large, $c_*/d \approx 10$ (i.e. some tens of grain diameters). It is interesting to reflect that whereas most theoretical treatments of T -curve behaviour focus almost exclusively on the former, it is the latter that is the key contributing factor to the tolerance in our material, by virtue of its controlling influence on

the scale of the flaw insensitivity range $c'_0 \leq c_0 \leq c''_0$ (Fig. 4). Thus whereas many materials processors seek to optimize only the magnitude T_∞/T_0 , it is apparent that the range c_*/d may be at least as important.

The type of construction depicted in Figs 4 to 6 is just one of several possible ways [6] of representing the T -curve influence on flaw mechanics. One commonly used, alternative construction warrants special mention, because of an unwitting tendency for workers in the ceramics field to regard its scope of application as universal. We refer to the construction in which both T and K_a are plotted as a function of crack extension, $\Delta c = c - c_0$ (or, for pores, $\Delta c = c - b_0$), instead of absolute crack size, c [17]. In that scheme a change in flaw size is represented as a shift in the intercept of the $K_a(\Delta c)$ load line along the negative Δc coordinate, with an invariant T - or R -curve fixed at some origin along the abscissa. Such a construction might at first sight appear to be equivalent to that shown in Fig. 5 (and 6) for defects without T -curve history over their initial area; there we simply displaced the origin of T instead of K_a . However, we recall from Sections 2.3 (and 2.4) that the function $T_\mu(\Delta c)$ (inserting $c = \Delta c + c_0$ in Equation 5, or $c = \Delta c + b_0$ in Equation 8) is not invariant with c_0 (or b_0); i.e. the shape of the T -curve depends on the initial flaw size. The alternative construction is even more inapplicable to flaws with full T -curve history, such as the microcrack system in Fig. 4, where the relative locations of the T and K_a origins are fixed regardless of c_0 . For this last flaw type, constructions that shift the relative K_a origin will inevitably lead to a significant underestimate of the tolerance level (e.g. will predict a curve closer to B than to A in Fig. 7). It is clear that considerable care needs to be exercised in drawing conclusions regarding strength characteristics from the traditional R -curve representations.

We have seen that the tolerance properties of a material with T -curve behaviour depend strongly on the flaw type. This dependence may be usefully explored in the indentation-strength test, by examining the data set in the low-load region. Thus we note for our alumina material in Fig. 2 that the $\sigma_m(P)$ data tend asymptotically to the strength level for breaks from natural flaws; and, moreover, that this level itself corresponds (within experimental scatter) to the plateau value σ_m^P in Fig. 7 for microcrack-type flaws with full T -curve history. We conclude that the dominant natural flaws in our alumina must have evolved within the (bridging) T -curve field, and are therefore most likely to be the grain-facet microcracks of the kind shown in Fig. 3a. There is indeed evidence from *in situ* observations of polished alumina surfaces that such microcracks are the most prevalent source of natural failures [7, 18]. That the $\sigma_m(P)$ plot for the indentation flaws is asymptotic to rather than coincident with the σ_m^P plateau is attributable to an additional driving force, proportional to P , associated with residual contact stresses [7, 10–12]. For flaws without complete T -curve history, e.g. the pores in Fig. 3b, the attendant reduction in strength values will manifest itself as a cut-off in the $\sigma_m(P)$ plot in the low-load region. This indicates that such defects are not present in a sufficient

number of specimens to lower the mean strengths of our alumina significantly, but there are reported data for several other ceramics without strong *T*-curve characteristics (including aluminas) that exhibit strong cut-off behaviour [7]. It is these latter defect types that pose the greatest threat to degradation of strength properties.

In conclusion, flaw insensitivity is a natural consequence of *T*-curve behaviour. The degree of insensitivity depends on such matters as history and geometry. The implications concerning materials design are profound. Nowhere is this more apparent than in ceramics processing strategy. Elimination of all flaws need not be the ultimate objective of materials fabrication. In this view it might not make good sense to pursue unlimited refinement of the microstructural makeup, particularly where the elements of that particular microstructure compensate by enhancing the *T*-curve. Moreover, the attendant crack stabilization afforded by the rising *T*-curve could be turned to advantage, to provide early warning of any impending failure [11]. It is clear that future decisions in ceramics design will inevitably require a proper understanding of the underlying mechanics of the *T*-curve response, along with a complete characterization of the flaw types that are most likely to lead the material system to failure.

Acknowledgements

The authors thank M. J. Readey, A. H. Heuer, J. Sibold, H. M. Chan and R. F. Cook for useful discussions on aspects of this work, and J. L. Runyan for experimental assistance. Funding was provided by the US Air Force Office of Scientific Research.

References

1. F. F. LANGE, *J. Amer. Ceram. Soc.* **66** (1983) 396.
2. F. F. LANGE and M. METCALF, *ibid.* **66** (1983) 398.

3. F. F. LANGE, B. I. DAVIS and I. A. AKSAY, *ibid.* **66** (1983) 407.
4. N. McN. ALFORD, J. D. BIRCHALL and K. KENDALL, *Nature* **330** (1987) 51.
5. K. R. VENKATACHARI and R. RAJ, *J. Amer. Ceram. Soc.* **70** (1987) 514.
6. Y.-W. MAI and B. R. LAWN, *Ann. Rev. Mater. Sci.* **16** (1986) 415.
7. R. F. COOK, B. R. LAWN and C. J. FAIRBANKS, *J. Amer. Ceram. Soc.* **68** (1985) 604.
8. R. W. STEINBRECH, R. KNEHANS and W. SCHARWACHTER, *J. Mater. Sci.* **18** (1983) 265.
9. P. L. SWANSON, C. J. FAIRBANKS, B. R. LAWN, Y.-W. MAI and B. J. HOCKEY, *J. Amer. Ceram. Soc.* **70** (1987) 279.
10. Y.-W. MAI and B. R. LAWN, *ibid.* **70** (1987) 289.
11. B. R. LAWN and C. J. FAIRBANKS, in "Review of Progress in Quantitative NDE", Vol. 6B, edited by D. O. Thompson and D. E. Chimenti (Plenum, New York, 1987) p. 1023.
12. R. F. COOK, C. J. FAIRBANKS, B. R. LAWN and Y.-W. MAI, *J. Mater. Res.* **2** (1987) 345.
13. K. KENDALL, N. McN. ALFORD, S. R. TAN and J. D. BIRCHALL, *ibid.* **1** (1986) 120.
14. R. F. COOK and D. R. CLARKE, *Acta. Metall.* **36** (1988) 555.
15. P. W. SWANSON, in "Fractography of Glasses and Ceramics", "Advances in Ceramics", Vol. 22 (American Ceramic Society, Columbus, Ohio, 1988) Ch. 23.
16. D. K. SHETTY, A. R. ROSENFELD and W. H. DUCKWORTH, in "Fracture Mechanics of Ceramics", Vol. 5, edited by R. C. Bradt, A. G. Evans, D. P. H. Hasselman and F. F. Lange (Plenum, New York, 1983) p. 531.
17. D. BROEK, "Elementary Engineering Fracture Mechanics" (Martinus Nijhoff, The Hague, 1983) Ch. 5.
18. R. W. STEINBRECH and O. SCHMENKEL, *J. Amer. Ceram. Soc.* **71** (1988) C-271.

Received 15 August

and accepted 19 December 1988